# Spectral dynamics analysis of ultra-line-narrowed $F_2$ laser

Takahito Kumazaki[*b], Osamu Wakabayashi[b], Ryoichi Nohdomi[d], Tatsuya Ariga[b], Hidenori Watanabe[d], Kazuaki Hotta[c], Hakaru Mizoguchi[d], Hiroki Tanaka[f], Akihiko Takahashi[e], Tatsuo Okada[f]

[a]Association of Super-Advanced Electronics Technologies, 1200 Manda, Hiratsuka-shi, Kanagawa 254-8567, Japan

[b]Komatsu Ltd., 1200 Manda, Hiratsuka-shi, Kanagawa 254-8567, Japan

[c]Ushio Inc., Asahi Tokai Bldg., 2-6-1 Ohtemachi, Chiyoda-ku, Tokyo 100-0004, Japan

[d]Gigaphoton Inc., 400, Yokokurashinden, Oyama-shi, Tochigi 323-8558, Japan

[e]Kyushu University School of Health Sciences, 3-1-1 Maidashi, Higashi-ku, Fukuoka 812-8582, Japan

[f]Kyushu University, 6-10-1 Hakozaki, Higashi-ku, Fukuoka 812-8581, Japan

## ABSTRACT

We have developed an ultra-line-narrowed, high-repetition-rate, high-power injection-locked $F_2$ laser system for 157 nm dioptric projection systems under the ASET project "$F_2$ Laser Lithography Development Project". A spectral bandwidth of < 0.2 pm (FWHM), an output power of > 25 W, and an energy stability (3-sigma) of < 10 % at 5 kHz repetition rate was successfully obtained by using a low-power ultra-line-narrowed oscillator laser and a high-gain multi-pass amplifier laser. These parameters satisfy the requirements of exposure tools. A numerical simulation code that can simulate the spectral dynamics of the $F_2$ laser under different operation modes such as free running operation, line-narrowed operation, and injection-locked operation, has also been developed. Using this simulation code, it is found that the instantaneous spectral bandwidth narrows monotonously during the laser pulse, and a narrower spectral output can be obtained by seeding the tail area of the line-narrowed $F_2$ laser pulse. And the line-narrowing operation of the oscillator laser and the behavior of the injection-locked laser system can be predicted very precisely with this simulation code. The development of $F_2$ laser for microlithography will be accelerated by this new simulation code.

**Keywords:** $F_2$ laser, 157 nm microlithography, line-narrowing, injection locking, spectral bandwidth, numerical simulation, rate equation, photon transport equation, MOPA

## 1. OUTLINE OF THE DEVELOPMENT

Basically two optical projection designs exist for 157 nm exposure tools to be used for 65 nm node lithography: dioptric and catadioptric. The relation between the laser spectral bandwidth and the laser output power necessity for two projection designs is shown in Figure 1. The catadioptric design uses mirrors, which avoid wavelength dispersion. Therefore, the catadioptric design has a much larger margin for the spectral bandwidth of the light source. The catadioptric design requires a bandwidth of 0.8 ~ 1.2 pm in full width at half maximum (FWHM) at 157 nm. For the dioptric design the chromatic aberration has to be corrected by applying at least two different lens materials: for example $CaF_2$ and $BaF_2$[1]. Alternatively, an

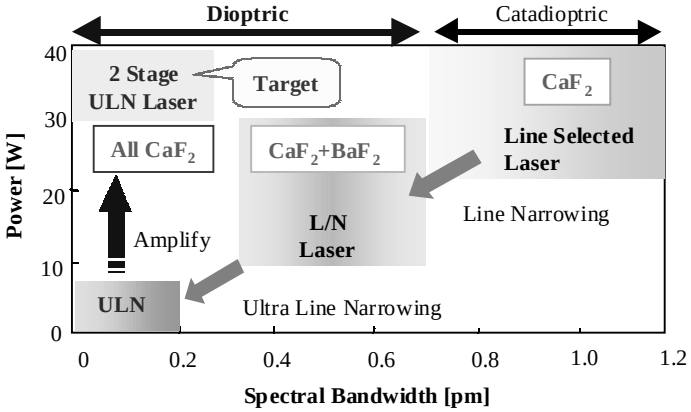


Figure 1: Laser type, spectral bandwidth and projection design

* T. Kumazaki; takahito_kumazaki@komatsu.co.jp; phone +81-463-35-9234; fax +81-463-35-9288

ultra-line-narrowed $F_2$ laser has to be used. The spectral bandwidth (FWHM) and the spectral purity, the bandwidth containing 95 % of the spectral energy, have to be < 0.2 pm and < 0.5 pm respectively. A high throughput requires a repetition rate of 5 kHz. Due to optical losses in the exposure tool, a laser pulse energy of 5 mJ is necessary. An energy stability below10 % (3-sigma) and wavelength stability below +-0.05 pm are also required for stable microlithography processing. However, it is quite difficult to achieve efficiently such a high output power and an ultra-line-narrowed bandwidth simultaneously due to existence of Amplified Spontaneous Emission (ASE) and due to the small number of round trips available. We solved this problem by developing an injection locked laser system: a low power oscillator laser with an ultra-line-narrowed bandwidth and a power amplifier laser, which has a resonator.

In addition, to understand the spectral dynamics of a line-narrowed $F_2$ laser and to obtain a design guideline for an optimized laser system, we have also been developing a numerical simulation code that calculates laser pulse shape and spectral bandwidth. The simulation results are compared with experiments.

## 2. SYSTEM CONFIGURATION

A photograph of the laser system[2] is shown in Figure 2. A prism-grating arrangement is used for line narrowing in the oscillator laser. The prisms are made from $CaF_2$ and their optical surfaces were all Anti-Reflection (AR) coated. The output coupler (OC) of the oscillator laser is a flat mirror with 10 % reflectance. For the amplifier laser, an unstable resonator of magnification 5 is adopted. The rear mirror of the unstable resonator has a hole in the center to pass the seed laser beam of the oscillator. The output coupler of the amplifier laser has a high-reflection (HR) coating in the center region and an AR coating in the outer region that transmits the amplifier laser. By using jitter reduced synchronization controller, the discharge delay time between the oscillator laser and amplifier laser can be adjusted. Both resonator mirrors of the amplifier laser are removed when we measure the saturation characteristics. This configuration is called Master Oscillator Power Amplifier (MOPA). The chambers have side windows to monitor the fluorescence sidelight. A high-resolution spectrometer and a high-resolution absolute wavelength meter were used to measure the spectral performance[3, 4, 5]. The instrument function of the spectrometer was measured with a 157 nm coherent light source[6] and its FWHM was about 0.1 pm. The wavelength meter uses a bromine lamp[7] as a wavelength standard. Laser pulses and fluorescence sidelights were detected by a bi-planar phototube. The pulse-to-pulse energy stability is measured by a VUV-sensible PIN-photodetector.

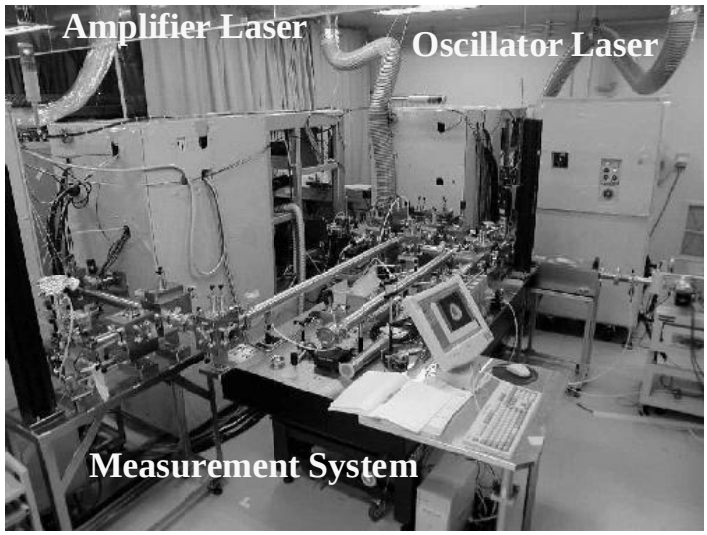


Figure 2: Photograph of the ultra-line-narrowed $F_2$ laser system

All the system is interconnected with a $N_2$ purged beam delivery unit to avoid oxygen and other gas contamination.

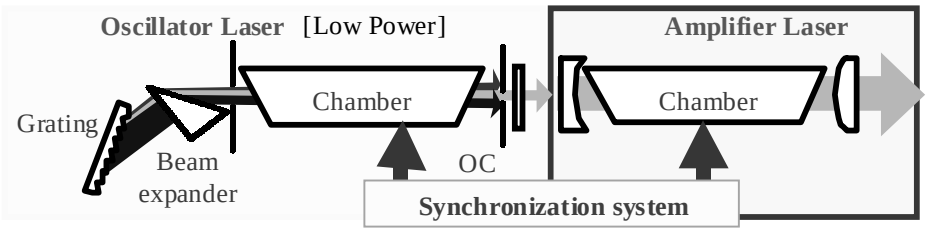


Figure 3: Laser system configuration

## 3. NUMERICAL SIMULATION

### Outline of the code

The numerical simulation code consists of

(1) the electrical circuit code, which describes the discharge circuit of the $F_2$ laser

(2) the Boltzmann code, which calculates the electron energy distribution function

(3) the rate equation code, which treats collisional excitations and de-excitations between particles and the emission and the absorption of photons

(4) the photon transport code, which describes the light amplification by the stimulated emission inside the laser cavity

Although self-consistent results can be obtained by coupling the above four codes[8], it is difficult to obtain accurate results. This is partly due to the fact that there are many unmeasured parameters of the $F_2$ molecule and the collision processes. For instance, even the collisional decay rate of the lower laser state, that greatly affects the laser operation through the so-called bottleneck effect, has not been measured.

To obtain more practical results, experimental results such as the fluorescence sidelight and the pulse shape under free running operation of $F_2$ laser were combined with the simulation code. $F_2$ lasers are considered to be a two-level laser system. The temporal pulse shape of the pumping rate is approximated with that of the fluorescence sidelight of the laser, although the pumping rate can be obtained by solving the Boltzmann code, the circuit code and the rate equation code.

### Rate equation and the photon transport equation

We define $I^+$ and $I^-$ as the power density of the laser beam at a wavelength $\lambda$ that propagates forward and backward in the resonator respectively. Setting the *z*-axis along the optical axis of the resonator, it was assumed that the optical intensity in the plane perpendicular to the *z*-axis was uniform. We also assume that the pressure broadening homogeneously broadens the fluorescence spectrum of the $F_2$ molecule. Based on the above model, $I^{\pm}$ satisfy the following rate equation [Eq. (1)(2)] and the photon transport equation [Eq. (3)].

$$\frac{\partial N_2(z,t)}{\partial t} = P(t) - \left[N_2(z,t) - N_1(z,t)\right] \times \sum_{\lambda} \frac{\sigma(\lambda)}{h\nu}\left[I^+(\lambda,z,t) + I^-(\lambda,z,t)\right] - \frac{N_2(z,t)}{\tau_2} - Q_2(t)N_2(z,t) \qquad (1)$$

$$\frac{\partial N_1(z,t)}{\partial t} = \left[N_2(z,t) - N_1(z,t)\right] \times \sum_{\lambda} \frac{\sigma(\lambda)}{h\nu}\left[I^+(\lambda,z,t) + I^-(\lambda,z,t)\right] + \frac{N_2(z,t)}{\tau_2} - Q_1(t)N_1(z,t) \qquad (2)$$

$$c\frac{\partial I^{\pm}(\lambda,z,t)}{\partial z} \pm \frac{\partial I^{\pm}(\lambda,z,t)}{\partial t} = c\left\{\left[N_2(z,t) - N_1(z,t)\right]\sigma(\lambda) - \alpha\right\} I^{\pm}(\lambda,z,t) \qquad (3)$$

$N_1$ and $N_2$ are the population densities of the lower and upper laser-states, respectively. $\sigma$ is the stimulated emission cross section, $\alpha$ is the additional absorption loss, $P$(t) is the pumping rate, $Q_1$ and $Q_2$ are the relaxation rates of the lower and upper states. $\tau_2$ is the radiative lifetime of the upper state.

### Numerical calculation and parameters

For the numerical calculations, the resonator was divided into many cells with a thin thickness along the *z*-axis. In addition, in each cell, the beam was divided into a large number of groups with respect to the wavelength with a width of $\Delta\lambda$, in order to calculate an oscillation spectrum. Then the set of the rate equations and the photon transport equation were solved by the Runge-Kutta method and the finite difference method. The radiative lifetime was taken from ref. 9.

The stimulated emission cross section of the $F_2$ molecules can be calculated based on the saturation measurements described below. The relaxation rate of the upper state $Q_2$ was calculated separately using the circuit code, the Boltzmann code and the rate equation code. The waveform of $P$(t) was approximated by the measured fluorescence sidelight without cavity mirrors, and its peak value $P_0$ and the relaxation rates of the lower state $Q_1$ are adjusted so that the calculated laser pulse shape agrees with the experimental one for free running operation.

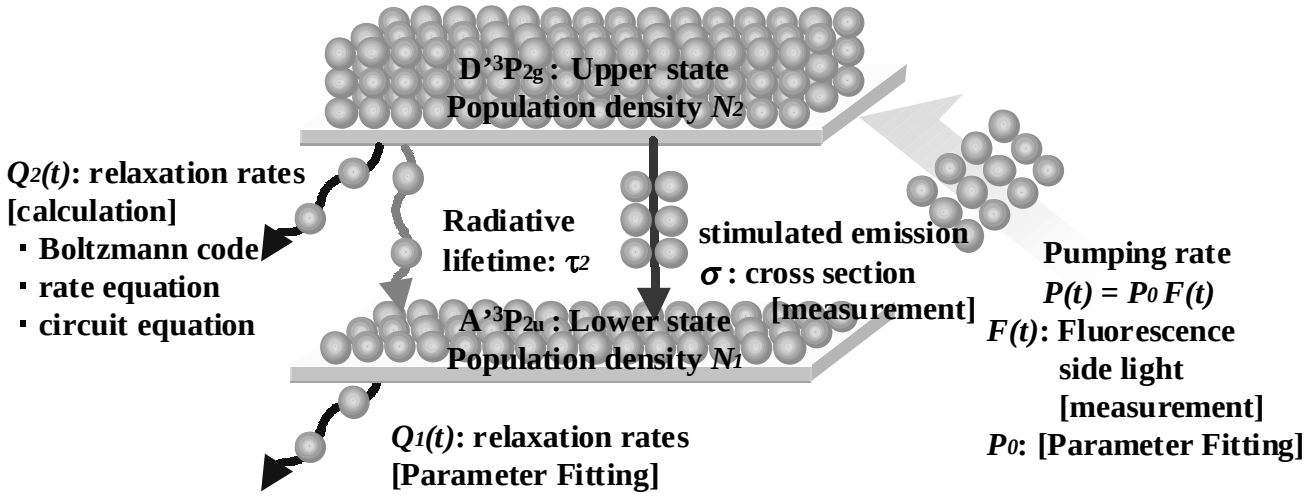


Figure 4: Laser model for simulation code

## 4. SYSTEM PERFORMANCE

### 4. 1 Single laser performance and jitter

The gas condition of the oscillator laser is optimized gas condition to get a line-narrowed bandwidth effectively. A too high gain operation causes undesirable ASE. The measured bandwidth FWHM of the oscillator laser is 0.24 pm. The true laser bandwidth FWHM is 0.17 pm, which is estimated by deconvolving the instrumental function. The output energy of the oscillator laser is 0.45 mJ. The line narrowing efficiency, defined by [line narrowed energy] / [free running energy], is about 25 %. The output energy of the amplifier laser without seeding is about 5 mJ.

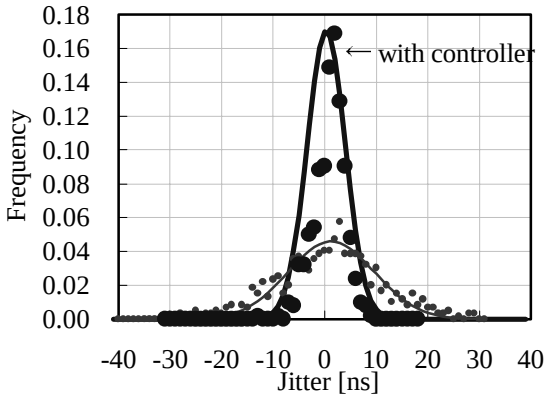


Figure 5: delay time fluctuation between lasers

Jitter control is one of the major issues for a synchronization system. For example, if the power supply has a charging stability of about 0.5 %, the discharge fluctuation will be around 20 ns for a single laser. Without the jitter controller, the fluctuation of the delay time was about +-30 ns. With the newly developed jitter compensation controller, the fluctuation of the delay time jitter is reduced to below +-10 ns at 5000 Hz. Figure 5 shows the delay time fluctuation between the oscillator and the amplifier laser.

### 4. 2 Saturation characteristics

The output energy dependence on the input energy of the injection locked and MOPA system is shown in Figure 6. Here, MOPA is examined to know the stimulated emission cross section. For the injection locked system, a very low injection energy density of about 0.01 mJ/cm$^2$ is required to saturate the output energy. Since this is small compared to the oscillator performance, stable system operation is possible.

Based on an analytical result[10] concerning saturation effects in lasers, the following equation connecting input power $I_{in}$ and output power $I_{out}$ is obtained when the input laser is amplified by a power amplifier, which has a small signal gain coefficient $g_0$ and gain length $L$.

$$\ln(I_{out} - I_{in}) = g_0 L - (I_{out} - I_{in}) \times \frac{\sigma \tau_2}{h\nu} \tag{4}$$

The stimulated emission cross section is estimated by the slope of Figure 7, and this result is used in the following numerical simulation, although it also can be obtained by the shape of the fluorescence spectrum.

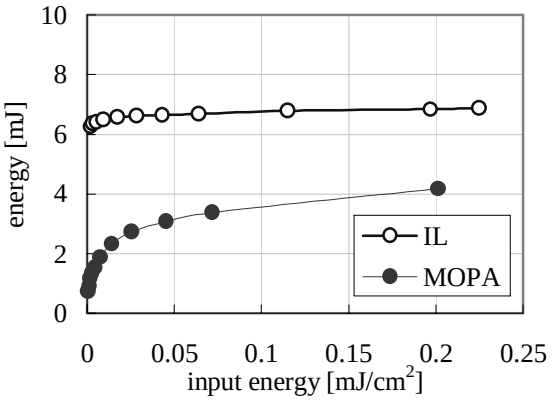


Figure 6: output energy versus input energy

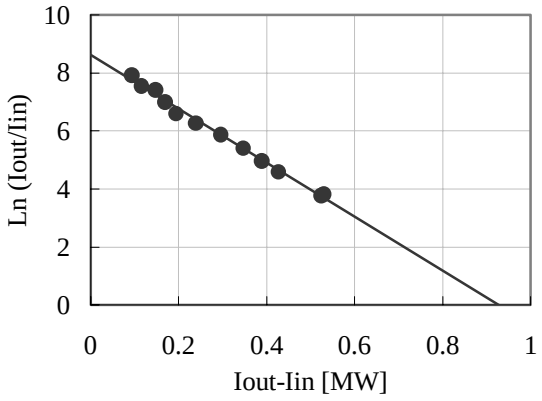


Figure 7: MOPA saturation characteristics

### 4. 3 Energy performance

The term "delay time" defines the time delay between the amplifier laser and oscillator laser. With increasing delay time, the tail of the oscillator laser pulse is injected into the amplifier laser.

The energy and the energy stability at 5000 Hz operation are shown in Figure 8. For a delay time above 50 ns the output energy decreases due to the reduction of the injection power. Over 50 ns time range both target values, > 5mJ and < 10 %, is satisfied.

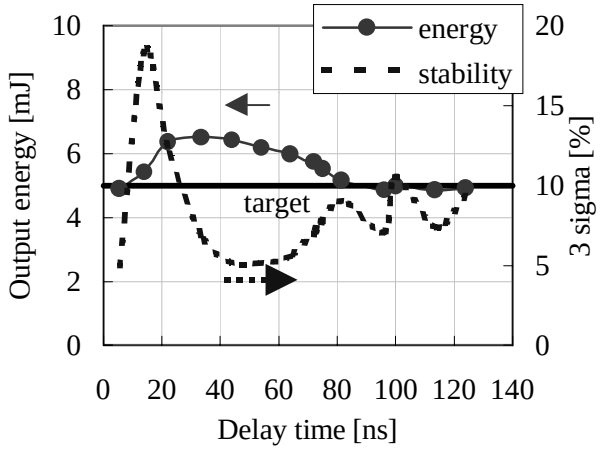


Figure 8: energy and energy stability versus delay time

### 4.4 Spectral performance

Figure 9 shows the deconvolved spectral bandwidth versus delay time. The bandwidth narrows with increasing delay time, because the injected oscillator bandwidth becomes narrower due to increasing round-trips. The bandwidth is less 0.2 pm for a time range of about 60 ns. The oscillator laser pulse intensity is not high enough to narrow the amplifier laser spectral bandwidth after 100 ns time delay and the bandwidth increases again. The typical spectral shape at a delay time of 62 ns is shown in Figure 10. Deconvolved spectral bandwidth and purity are 0.12 pm, 0.45 pm, and are narrower than that of the oscillator laser.

The performance of the laser system target and result is summarized in table 1. We have successfully cleared all target parameters.

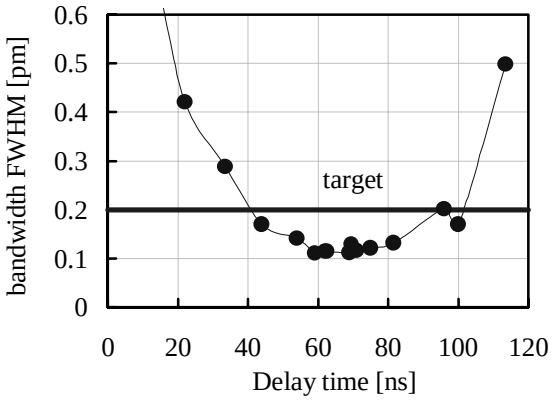


Figure 9: spectral bandwidth versus delay time

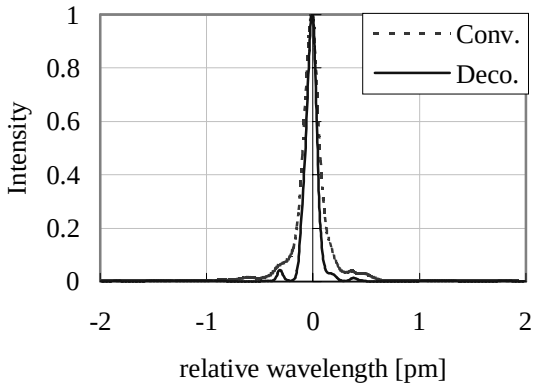


Figure 10: spectra of the laser system

| Parameters | Target | Result |
|---|---|---|
| Repetition Rate | 5000 Hz | 5000 Hz |
| Pulse Energy | 5 mJ | 6 mJ |
| Average Power | 25 W | 30 W |
| Energy Stability (3-sigma) | 10 % | 5.6 % |
| Spectral Bandwidth (FWHM) | 0.2 pm | 0.12 pm |
| Spectral Purity (95%) | 0.5 pm | 0.45 pm |
| Wavelength Stability | +- 0.05 pm | +- 0.04 pm |

Table 1: target and result performance of the laser system

## 5. SIMULATION COMPARED WITH EXPERIMENT

In this section, the results of the numerical simulation for free running operation, line-narrowed operation, and injection locked operation are shown and compared to the experimental results that are measured by the described system.

### 5. 1 Free running operation

In free-running operation mode, a stable resonator with flat output coupler and HR mirror is used. The fitting parameters, $P_o$ and $Q_1$, are adjusted to have good agreement with the experiment. Best-parameter-fitted simulated laser pulse shape is shown in Figure 11. These fitted values are used for all cases. The behavior of ASE is also shown as a reference.

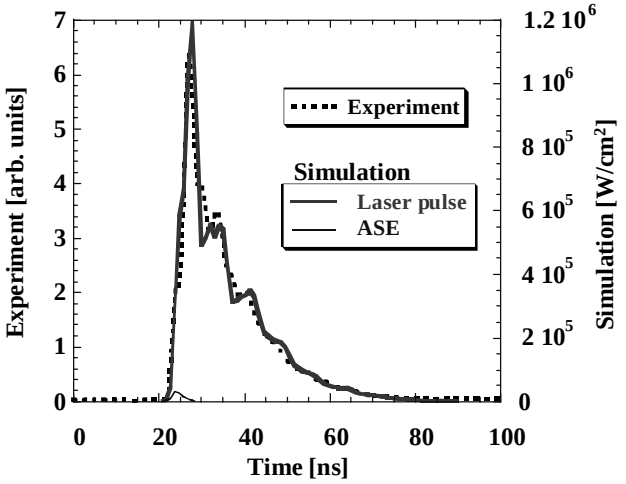


Figure 11: Laser pulse shapes in free running operation

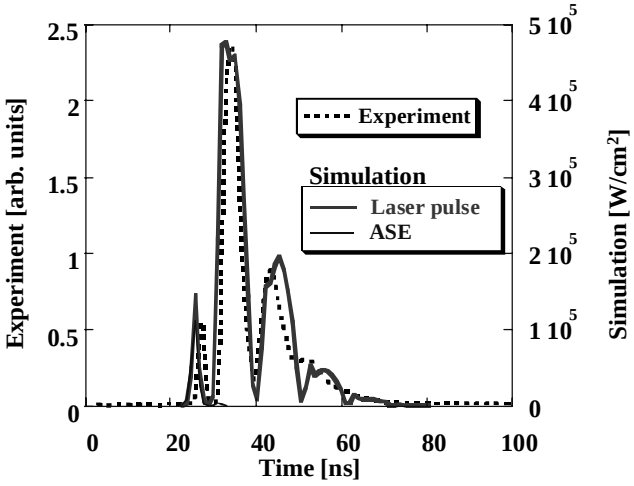


Figure 12: Laser pulse shapes in line narrowed operation

### 5. 2 Line-narrowed operation

In this calculation, the wavelength dependence was taken into account. The cavity length was also changed to that of the line-narrowed $F_2$ laser. The calculated laser pulse waveform is shown in Figure 12, along with the experimental one. Both oscillation pulse shapes well coincide. Thus, it was confirmed that the present method is able to accurately predict the laser pulse shape. The temporal change of the spectral bandwidth FWHM during laser pulse is shown in Figure 13 and compared with the measured time-resolved spectral bandwidth, which is taken by the high-resolution spectrometer equipped with a streak camera. Due the relatively weak signal, the convolution value is, however, used for comparison. As shown in Figure 13, the spectral bandwidth decreases with increasing photon round-trips in the line-narrowing resonator.

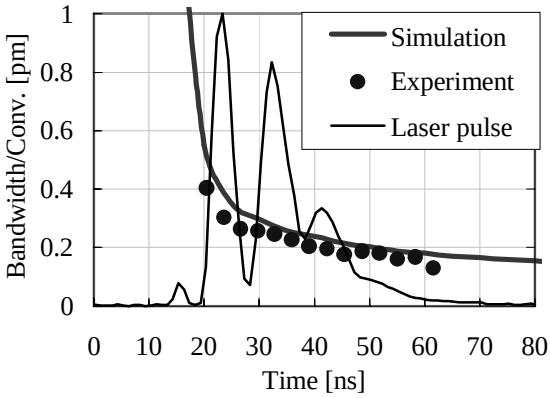


Figure 13: instantaneous bandwidth of the oscillator

### 5. 3 Injection-locked operation

Next, the injection-locked operation was simulated. The line-narrowed laser beam from the oscillator laser is injected into the amplifier's cavity that can provide appreciable output energy. In the numerical simulation of the injection-seeded operation, the pulse shape and the spectral charcteristics of the seeder were adopted as follows. For the pulse shape, the experimental pulse shape was used. We assumed that the bandwidth of the seeder decreased with time as obtained by the simulation in Figure 13. This seed pulse was added to the 1st sub-cell of the amplifier laser cavity in the calculation. A similar behavior as in Figure 9 is obtained for the spectral performance.

It is very important to note that the time-integrated bandwidth of the amplifier laser can be narrower than that of the oscillator laser by optimizing the seed timing. The integrated bandwidth of the oscillator laser has not to be < 0.2 pm. Only the time-resolved bandwidth of the injection laser pulse should be < 0.2 pm, in order to achieve < 0.2 pm with the synchronization system.

## 6. CONCLUSION

For a wide time range of 50 ns, an energy of > 5 mJ and an energy fluctuation (3-sigma) < 10 % was obtained with satisfying spectral performance. We conclude that the key technologies for an ultra-line-narrowed injection locked $F_2$ laser system have been developed and that the system is a promising light source candidate for 157 nm dioptric projection systems. A numerical simulation has also been developed, in order to investigate the spectral dynamics of a line-narrowed $F_2$ laser. The simulated results show good agreement with the experiment. Using this code, the development of an ultra-line-narrowed $F_2$ laser for microlithography will be accelerated.

## ACKNOWLEDGMENTS

A part of this work was performed under the management of Association of Super-Advanced Electronics Technologies (ASET) in the Ministry of Economy, Trade and Industry (METI) Program supported by New Energy and Industrial Technology Development Organization (NEDO).

## REFERENCES

1. J. H. Burnett, R. Gupta, and U. Griesmann, Appl. Opt. **41** p. 2508, 2002
2. T. Ariga, H. Watanabe, T. Kumazaki, N. Kitatochi, K. Sasano, Y. Ueno, M. Konishi, T. Suganuma, M. Nakano, T. Yamashita, T. Nishisaka, R. Nohdomi, K. Hotta, H. Mizoguchi, and K. Nakao, "Development of a 5 kHz Ultra-Line-Narrowed $F_2$ Laser for Dioptric Projection Systems", Proc. SPIE Vol. *4691*, pp.652-659, 2002
3. O. Wakabayashi, J. Sakuma, T. Suzuki, H. Kubo, N. Kitatotchi, T. Suganuma, T. Nakaike, T. Kumazaki, Kazuaki Hotta, H. Mizoguchi and K Nakao, "Spectral Measurement of Ultra Line-Narrowed $F_2$ Laser", Proc. SPIE Vol. *4346*, pp. 1066-1073, 2001
4. J. Fujimoto, T. Nakaike, T. Suzuki, S, Nagai, T. Yabu, G. Soumagne, T. Chiba, O. Wakabayashi and H. Mizoguchi, "Spectral characteristics of the molecular fluorine laser", SEMATEC 2nd international Symposium on 157nm Lithography Digest Abstracts, 2001
5. T. Nakaike, O. Wakabayashi, T. Suzuki, H. Mizoguchi, K Nakao, R. Nohdomi, T. Ariga, N. Kitatochi, T. Suganuma, T. Kumazaki, K. Hotta and M. Yoshioka, "Spectral Metrologies for ultra-line-narrowed $F_2$ laser", Proc. SPIE Vol. *4691*, pp.1714-1721, 2002
6. T. Suganuma, H. Kubo, O. Wakabayashi, H. Mizoguchi, K. Nakao, Y. Nabekawa, T. Togashi and S. Watanabe, "157-nm Coherent Light Source for $F_2$ Laser Lithography [CPD7-1]", *CLEO 2001Postdeadline Papers*, 2001
7. M. Yoshioka, T. Kitagawa, T. Arimoto, H. Matsuno, T. Hiramoto, T. Suzuki and K. Hotta, "Br Lamp for $F_2$ Laser Wavelength Calibration", Proc. SPIE Vol. *4346*, pp 1238-1243, 2001
8. M. Kakehata, T. Uematsu, F. Kannari and M. Obara, IEEE J. Quantum Electron. **27** 2456, 1991
9. M. Diegelmann, K. Hohla, F. Rebentrost, K. L. Kompa, J. Chem. Phys. **76** 1233, 1982
10. W. W. Rigrod, "Saturation Effects in High-Gain Lasers", J. of Appl. Phys, vol. **36**, pp.2487-2490, Aug. 1965